The International Journal of Advanced Manufacturing Technology (2022) 121:5971–5990
https://doi.org/10.1007/s00170-022-09655-6

ORIGINAL ARTICLE

Development of a fuzzy-AHP system to select the printing method for polycaprolactone (PCL)-based scaffolds

Lan Xuan Phung[1] · Truong Do[2] · Phuong Tran[3] · Trung Kien Nguyen[1]

Received: 13 April 2022 / Accepted: 2 July 2022 / Published online: 23 July 2022

Abstract

Polycaprolactone (PCL)-based scaffolds have great potential in various tissue engineering applications because of their biodegradability, high mechanical strength, and easy fabrication using different 3D printing methods. However, previous research has only focused on developing and examining each PCL-based scaffold printing method's merits and limitations separately. Thus, the lack of a systematic comparison of the various methods to recommend the most appropriate one for each application remains. This paper provides an overview of different PCL-based scaffold printing methods. Four typical 3D printing methods for fabricating PCL-based scaffolds and five important evaluation criteria including quality, usage, productivity, cost, and flexibility are identified. The integrated fuzzy-analytical hierarchy process (i-FAHP) and sensitivity analysis are proposed as multi-criteria decision-making methods for selecting the most appropriate scaffold printing method (SPM) under constrained construction and material types. Customized software based on a flexible fuzzy-AHP expert system is built to support decision-makers in determining the optimal SPM quickly and effectively. The result shows that the melt-based extrusion method is optimal for different scaffold types. This study's findings will be useful for developing biomaterial and multi-head 3D bioprinters for customized and commercial tissue engineering applications.

Keywords Fuzzy-AHP · 3D printing · Scaffold fabrication · Tissue engineering · PCL-based material

1 Introduction

Additive manufacturing (AM) refers to the technologies that build 3D objects by adding material layer-by-layer. Common approaches to AM include photochemical transformation (stereolithography — SLA), thermal transformation (fused deposition modeling — FDM), binding by heat treatment (selective laser sintering — SLS), and binding/adhesion (three-dimensional printing — 3DP) [1]. Currently, AM is widely accepted in various sectors as a prototyping tool and direct process to construct end-user products. Besides various well-known applications in engineering, industrial design, medical research, and education, additive manufacturing has assumed an important role in the future of healthcare, such as bioimplants, drug delivery, and tissue engineering [2, 3]. Tissue engineering involves scaffolds, cells, biomaterials, and bioactive factors to obtain functional and autologous tissues. A scaffold is a physical space for new tissue development, providing mechanical support, nutrients, and waste transportation. Additive manufacturing has a significant advantage for scaffold fabrication because of its geometric controllability. Such geometry factors include scaffold shape, line width, pore size, porosity, and interconnectivity which are important in imitating a tissue's morphology, biocompatibility, and mechanical properties [4].

PCL is an approved FDA polymer and the most common thermoplastic material for scaffold fabrication due to its high mechanical strength and good biodegradation characteristics among the synthesis polymers used in tissue engineering. By adjusting its molecular weight or combining it with other biomaterials to control its biodegradation time and biocompatibility, PCL can be used in various applications from hard to soft tissue engineering. PCL can also be used in separated

✉ Lan Xuan Phung
lan.phungxuan@hust.edu.vn

✉ Trung Kien Nguyen
trung.nguyenkien@hust.edu.vn

1 School of Mechanical Engineering, Hanoi University of Science and Technology, Hanoi 100000, Vietnam

2 College of Engineering and Computer Science, VinUniversity, Hanoi 100000, Vietnam

3 School of Engineering, RMIT University, Melbourne, Australia

printhead without cells for scaffold fabrication in multi-head bioprinting systems [5, 6].

Previous studies have introduced different additive manufacturing methods for fabricating PCL-based scaffolds. Because PCL is a thermoplastic material, conventional FDM (c-FDM) using filament is the most well-known, simple, and low-cost additive manufacturing technique for scaffold fabrication [7, 8]. In addition, other printing methods based on thermal transformation processes, such as screw-based extrusion (s-FDM) or melt-based deposition (m-FDM) using pellets or powders, have been preferably used for scaffold fabrication [9, 10]. Unlike the thermal transformation approaches, the solution extrusion technique shows the potential fabrication process for scaffold made of various biomaterials, such as hydrogel, thermoplastics, and combined biomaterials with desired geometric characteristics. The solvent-based dispenser (SBD) method uses solvents such as dichloromethane and chloroform, to dissolve thermoplastic polymer to make a solution before depositing it through a nozzle at room temperature [11, 12]. As there are several different scaffold printing methods (SPMs) with unique characteristics, it is required to determine the optimal method for specific purposes in tissue engineering applications.

Several experimental studies have compared the characteristics of scaffolds fabricated by several techniques. Patrício et al. compared two types of blend preparation, including melt blending and solvent casting, by evaluating the scaffold's geometry, thermal, chemical, mechanical, and biological properties [13]. The results showed that the solvent casting material preparation yielded better mechanical and biological characteristics than blended material prepared by melt blending. The scaffolds fabricated by the m-FDM and SBD methods are evaluated in terms of geometric characteristics, mechanical properties, degradation, and bioactivity [14]. The results indicated the potential of the SBD printing method in bioprinting applications. Zimmerling et al. discovered that the mechanical properties and accuracy of fabrication scaffold using m-FDM is higher than those with SBD [15]. While most studies have focused on the characteristics of the printed scaffolds using different printing methods, Andrea et al. presented an experimental protocol and a comparison among common SPMs including c-FDM, s-FDM, and m-FDM on several evaluation factors related to the printing process, such as thermal degradation, usage, material compatibility, material wastage, and working temperature [16]. c-FDM in comparison with s-FDM provides higher accuracy for fabrication scaffolds while s-FDM and m-FDM are more versatile than c-FDM in the ability to directly combine with other additives. m-FDM is more difficult to control the flow rate than others [16, 17].

Besides product quality and material characteristics, different aspects should be considered for various scaffold printing methods, such as productivity and process economy. These characteristics are commonly referred to in the evaluation of 3D printing methods or 3D printers [18–20]. 3D printing methods applied in tissue engineering also have typical requirements related to biocompatibility. These characteristics are sterilization, post-processing, toxicity, and bioprinting integration ability. However, most of the evaluation systems for SPMs do not fully achieve these characteristics. With various SPMs and different impacted factors, the selection of the most suitable method among all SPMs is time-consuming, and thus, it has become a challenging task for decision-makers in research and industry application.

Over the past three decades, the multi-criteria decision-making method (MCDM) has been widely used to solve different decision-making problems through alternative evaluations based on multi-criteria. In the mechanical engineering field, MCDM has been successfully applied in selecting optimal manufacturing process, 3D printing method, and machine tool [21–24]. Among all MCDM methods, the analytical hierarchy process (AHP) has been one of the most popular techniques for evaluating multiple attributes to select the optimal alternative. In this method, based on a pair-wise comparison between the alternatives and criteria from multiple expert judgments, the AHP method combines separate evaluations to obtain an overall priority rank of the alternatives considering multiple criteria. Recently, the AHP method has been applied to the additive manufacturing process or 3D printer selection [20, 22]. However, decision-makers find it difficult to choose the exact numerical values for pair-wise comparison judgments in the AHP model. Thus, the fuzzy-AHP method has been developed to overcome the limitations of the AHP method. In this method, the concepts of fuzzy set theory have been applied to change fixed value judgment into interval judgment. This method has been widely used in the additive manufacturing process and bioprinter selection [23, 25]. The conventional fuzzy-AHP method is typically applied to obtain the priority of alternatives for a specific condition. However, the conventional model is inappropriate for complex and flexible problems with different initial conditions.

This paper presents an i-FAHP model that combines the selection and evaluation criteria in a unique model to solve problems under various initial conditions. Firstly, critical factors are discovered after reviewing the existing literature and referring to experts. The characteristics of alternatives are investigated in detail by practical experience and a thorough literature review. Then, the hierarchy structure of the SPM model, including two selection criteria, five evaluation criteria and four alternatives is constructed. The pair-wise comparison matrices for criteria, sub-criteria, or alternatives are created and checked for the consistency of judgments. The overall priority of SPMs is generated for decision-makers with the help of a developed computer program. A sensitivity analysis is executed to determine the effectiveness and stability of the overall performance. While most studies have not systematically and comprehensively performed multi-criteria evaluations of SPMs for thermoplastic material in general, and PCL-based materials in particular, the system of i-FAHP corresponding with each specific application can provide flexible solutions and multi-criteria SPM selection for practical tissue engineering applications.

2 Literature review

2.1 Scaffold types

Three terminologies are used to describe the different constructions of scaffolds: general scaffold (GS), hybrid scaffold (HS), and hybrid constructs (HCs) [26]. Early development of PCL-based scaffold for tissue engineering, GS has been fabricated using 3D printers with a single printhead [8, 9, 27]. HS refers to those structures printed with multiple printheads without cells [28–31]. HC is constructed similarly to HS but has at least one printhead containing cells [26, 32]. For each printhead, the material can be pure PCL material, referred to as a single material (SM) in three forms: filament, pellet, or powder [27, 33, 34]. Other materials can be combined with PCL in one printhead using two methods: (a) making blended material (BM) by thermal treatment or solvent dissolution to form a unique and homogenous filament or pellet before feeding it into the printing system [9, 35]; (b) mixing at room temperature and directly supplying to the fabricating system, referred to as a mixture of materials or mixed material (MM) [36, 37]. Figure 1 summarizes the common scaffold types based on different construction and material types.

2.2 PCL based-scaffold printing methods

The four most popular methods used to produce scaffolds for tissue engineering are briefly reviewed from the existing literature and are reported as follows:

(a) ***Conventional fused deposition modeling (c-FDM)***
The c-FDM technique is one of the well-known 3D printing methods, which involves the melt extrusion of material in a filament form through a heated nozzle (Fig. 2a). The main advantages of the c-FDM technique are simple system design and operation, continuous material supply, less melted material, and improvement in control and accuracy [16]. Commercial or open-source 3D FDM printers can be used to construct GS using PCL filament [8, 38]. However, the lack of commercial PCL-based material in SM and BM filament form is the main disadvantage of the c-FDM method. To apply the c-FDM method for PCL-based materials, several studies have made their own filaments from commercial PCL pellets or powder from pure PCL pellets [39] or blended material such as PCL/TCP or PCL/HA/PLA [35, 38].

(b) ***Screw-based extrusion (s-FDM)***
The s-FDM method shown in Fig. 2b is developed with the primary material in the most common form as pellet or powder [40] to overcome the limitations of the c-FDM method. The melted material proceeds only in the region near the nozzle or in the whole barrel, depending on the barrel design [41]. The material flow is transferred to the nozzle by a screw's feeding, making the system complicated and difficult to take apart for cleaning. However, the system can directly use an original material form from suppliers without filament preparation. By directly adding other fillers

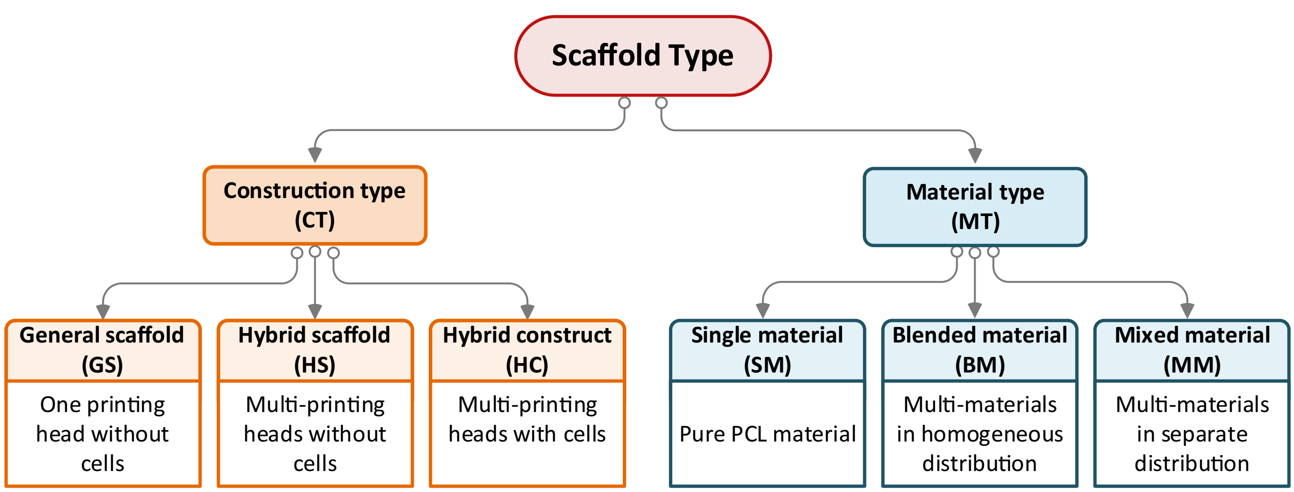

Fig. 1 Common scaffold types for tissue engineering applications

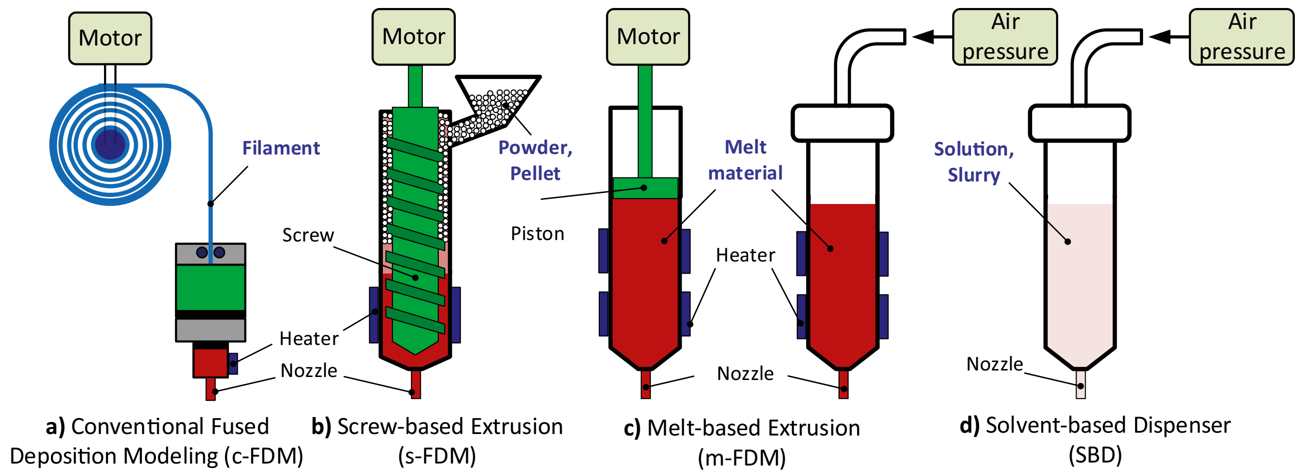

Fig. 2 Schematic of common scaffold fabrication methods for thermoplastic materials

into PCL powder, it can be easy to construct scaffolds from a mixture of materials such as PCL/TCP or PCL/HA [9, 36]. Most studies in the literature review have used c-FDM and s-FDM to fabricate scaffolds in GS type.

(c) ***Melt-based extrusion (m-FDM)***

The m-FDM method creates the material flow under pressure through the nozzle without using a screw-in barrel as demonstrated in Fig. 2c. Material can be melted directly in the barrel [42, 43] or heated before being fed into the barrel [28, 32, 44]. In the m-FDM system, the whole barrel is heated during the printing process, which can cause a thermal effect under prolonged heat exposure. A motor or air pressure can be employed to transfer the melted material into the nozzle; however, air pressure is mostly used. The m-FDM technique is commonly combined with other types of printheads to make HS and HC constructions. The m-FDM method is suitable for all material combination types, including SM, BM, or MM [6, 13, 45]. Material flexibility is the main advantage of this technique; however, flow rate control using air pressure is poor compared to the previous two techniques, resulting in lower product quality [16]. The cost of compressed air systems and control valves increases equipment investment. The three above methods all require high working temperatures depending on the melting point of the material mixture, which contributed to their main limitation in the fabrication of scaffolds.

(d) ***Solvent-based dispenser (SBD)***

An SBD produces a slurry or solution by dissolving thermoplastic material in a specific solvent, such as chloroform or dichloromethane, that is toxic for users in preparing the solution and can cause significant damage to cells. The working temperature is room temperature, which is the main advantage of this technique. The solution is deposited on the platform using air pressure. The literature review shows that the SBD technique has been used to fabricate all construction types with MM material [29, 37, 46]. Although the technique is easy to use and clean, post-processing is necessary to completely remove the solvent from the scaffold to prevent cytotoxicity [47]. Thus, the technique shows significant limitations with HC type. Shrinkage or swelling after removing the solvent is also a disadvantage of the SBD method [15].

In general, each SPM has specific merits and limitations and is sufficient for specific purposes. It is necessary to develop a systematic and objective approach for comparing various SPMs to derive the most suitable method for decision-makers corresponding to specific purposes. Table 1 summarizes the literature review of the four SPMs for various scaffold types. The literature review also helps to identify various significant factors for tissue engineering applications. The factors include printed scaffold accuracy such as the size and tolerance of the printed line width or pore, printing speed closely related to the printing time, working temperature, material compatibility, and an in vivo/in vitro study.

It also shows that m-FDM and SBD are common methods for HS. While m-FDM has been mostly used for HC, the c-FDM and s-FDM methods have been chosen for GS. However, such a common fact may have been due to the availability of SPMs in particular laboratories. Moreover, there was no specific assessment to compare and choose the appropriate solution. This research work will provide a systematic and multi-criteria evaluation method that allows decision-makers to select the proper SPM for their key research purpose. Based on the literature review, two selection criteria

Table 1 Review of printing methods for PCL-based material from different aspects

No	Material	Form	Construct-material types	Fabrication techniques	3D printer	Material preparation	Post processing	Line width (µm)	Pore size (µm)	Working temp	Printing speed (mm/s)	Printing tolerance	In vitro/in vivo study	Ref
1	PCL	Filament	GS_SM	c-FDM	MarkerBot Replicator	-	-	400	-	100	10	PS: 380 ± 1.2	-	[27]
2	PCL	Filament	GS_SM	c-FDM	FDM 3D Modeler RP system	Make blended filament	-	-	-	-	-	-	Osteoblasts and chondrocytes	[8]
3	PCL	Filament	GS_SM	c-FDM	Hephestos 2 Prusa i3	-	-	400	-	-	-	LW: 361 ± 26 PS: 816 ± 61	-	[48]
4	PCL/TCP	Filament	GS_BM	c-FDM	Sethi S3	Make blended filament	-	400	200	145	20	LW: 404 ± 10 PS: 186 ± 16	-	[35]
5	PCL/oyster shell	Filament	GS_BM	c-FDM	Weistek-WT1, Shenzhen	Make blended filament	-	400	600	120	7	LW: 465 ± 13 PS: 604 ± 28	MG63 osteoblast-like cells	[49]
6	PCL/HA/PLA	Filament	GS_BM	c-FDM	MakerBot Replicator 2	Make blended filament	-	-	-	210	60	-	Human osteosarcoma cells	[38]
7	PCL/TCP	Granules 0.5 mm	GS_MM	s-FDM	FabCTI 3D printer	-	-	400	-	105	12	LW: 447 ± 14 PS: 430 ± 79		[36]
8	PCL/HA	Pellet	GS_MM	s-FDM	Custom made	-	-	-	-	90	20	-	Fetal bovine osteoblast cells	[9]
9	PCL/graphene	Pellet	GS_BM	s-FDM	3D Discovery Bench-top	Make blended pellet	-	330	350	90	12	LW: 361.06 ± 22.71 PS: 340.05 ± 20.91	Human adipose-derived stem cells	[50]
10	PCL/MWCNT	Pellet	GS_BM	s-FDM	3D Discovery, RegenHU	Make blended pellet	-	330	350	90	20	LW: 312.2 ± 14.4 PS: 378.5 ± 14.6	Human adipose derived stem cells	[51]
11	PCL	Pellet	GS_SM	s-FDM	Custom made	-	-	-	-	110	1	-	-	[40]
12	PCL	Pellet	GS_SM	m-FDM	3D Discovery Bio- plotter	-	-	260	740	70	4	LW: 307 ± 14 PS: 660 ± 17	-	[33]
13	PCL/PEG	Pellet	GS_BM	m-FDM	-	Make blended pellet	-	500	500	65	15	LW: 440 ± 50 PS: 490 ± 30	Skin fibroblast cells	[52]
14	PCL/PLGA/TCP	Pellet	GS_MM	m-FDM	Custom made (MHDS)	Make melt material	-	200	600	120	1	LW: 200 ± 20 PS: 600 ± 20	hBMSCs	[32]
15	PCL	Pellet	GS_SM	m-FDM	Bioscaffolder device	-	-	300	300	90	4	LW: 253 ± 29 PS: 310 ± 24	MC3T3-E1 cells	[43]
16	PCL-(cell/alginate hydrogel)	Pellet	HC_SM	m-FDM	3D-BioplotterTM system	-	-	-	-	80	1		Chondrocyte bioink	[26]
17	PCL/PLA	Pellet	GS_BM	m-FDM	BioCell Printing system	Make blended pellet	-	350	350	-	-	LW: 434 ± 27 PS: 294 ± 12	MG63 osteoblast-like cells	[13]
18	PCL-(TGFb/alginate cell mixture)	Pellet	HC_SM	m-FDM	Custom made (MHDS)	-	-	200	400	80	1.2	LW: 200 ± 20 PS: 400 ± 20	Chondrocytes bioink	[6]
19	PCL/PLGA-hydrogel	Pellet	HS_MM	m-FDM	Custom made (MHDS)	-	-	-	-	120	2	-	MC3T3-E1 preosteoblasts	[28]

Table 1 (continued)

No	Material	Form	Construct-material types	Fabrication techniques	3D printer	Material preparation	Post processing	Line width (µm)	Pore size (µm)	Working temp	Printing speed (mm/s)	Printing tolerance	In vitro/in vivo study	Ref
20	PCL-GelMA	Powder	HS_SM	m-FDM	Bioplotter	-	-	-	-	160	2	-	DPSCs	[53]
21	PCL-collagen	Pellet	HS-SM	m-FDM	Custom made	-	-	350	-	130	-	LW: 378 ± 43 PS: 326 ± 31	MG63 cells	[30]
22	PCL/alginate (cell-laden	Pellet	HC_BM	m-FDM	DASA Robot	Make blended pellet	-	400	-	130	5	LW: ~ 500	Osteoblast-like-cells	[54]
23	PCL/gelatin/ sodium alginate	Pellet	HS_MM	SBD	Custom made	Dissolve in dichloromethane	Remove solvent	500	450	25	20	LW: 440 ± 41.19 PS: 527 ± 34.38	hASCs	[29]
24	PCL/HA	Pellet	GS_MM	SBD	-	Dissolve in GAC	Remove solvent	400	400	25	5	LW: 235 ± 43 PS: 212 ± 31	Bone MSCs	[55]
25	PCL/TCP/ collagen	Pellet	GS_MM	SBD	Hyrel 3D, SDS5 Extruder	Dissolve in dichloromethane	Remove solvent	-	-	35	50	-	Human osteosarcoma cells	[37]
26	PCL	Pellet	GS_SM	SBD	Ez-ROBO5, Iwashita,	Dissolve in Acetone	Remove solvent	400	-	RT	-	LW: 224 ± 9 PS: 986 ± 2	-	[34]
27	PCL/HA/CNT	Pellet	GS_MM	SBD		Dissolve in dichloromethane	Remove solvent	-	-	RT	-		MG63 osteoblast-like cells	[11]
28	PCL/13-93B3 glaGS_ (aglinate/ gelatin/ ASCs)	Powder	HC_MM	SBD	Modified Prusa I3A Pro	Dissolve in chloroform	-	300	-	RT	10	LW: 328 ± 36 PS: 314 ± 22	ASCs bio-ink	[56]
29	PCL/HA	Pellet	GS_MM	SBD	3D Bioplotter M	Dissolve in dichloromethane	-	510		RT	-	LW: 544 ± 64	-	[15]

have been proposed in this research work: construction type (CT) and material type (MT). While CT consists of three selection criteria: GS, HS, and HC, MT is a combination of materials that includes three material selections: SM, BM, and MM. Four approved alternatives are considered in this research work named c-FDM, s-FDM, m-FDM, and SBD.

3 Criteria descriptions

SPMs need to meet the common criteria of conventional 3D printing technology and be sufficient for specific goals, such as flexibility of methods, materials, and strict sterilization usage conditions in producing biological products. The following literature review is related to the criteria for evaluating the 3D printing methods, in particular the features of scaffold fabrication.

3.1 Product quality

Among the five criteria, product quality has assumed the most important role in selecting the printing method in previous studies [20, 57–59]. Briefly, product quality is related to the quality of the complete product produced by a 3D printing method, where accuracy and surface roughness are the most important factors [16, 59, 60]. Based on the literature review shown in Table 1, the average printing accuracy and printing speed of the different SPMs are calculated and presented in Table 2. The proposed printing accuracy (δ_{PA}) is derived from the printing ratio (δ_{PR}) and the printing error (δ_{PE}). δ_{PR} is determined from the difference between the line width of the design model and the printed model while δ_{PE} is related to the standard deviation of the printed line width or pore size. δ_{PA} can be calculated according to Eq. (1).

$$\delta_{PA} = \frac{\delta_{PR} + \delta_{PE}}{2} = \frac{\frac{|L_D - L_P|}{L_D} + \frac{2SD}{L_P}}{2}, \tag{1}$$

where: L_D is the line width of the design model; L_P is the line width of the printed model; SD is the standard deviation of the printed line. It can be observed in Table 2 that the c-FDM printing method obtained the printing model with the highest δ_{PA} and the SBD printing method had the lowest δ_{PA}. This outcome was mainly due to shrinkage after solvent removal during the post-processing stage. Andrea et al. showed that the printing temperature significantly affected flow rate, solidification, and geometric accuracy [16]. Material subjected to long exposure to high temperatures in the barrel would thermally degrade over time, affecting printed scaffolds' quality. A comparison of thermal degradation among the three SPMs based on the FDM technique was established in his research work. Thus, the thermal effect is considered an evaluation factor in selecting the optimal printing method for this research work. Among all methods, only the SBD method can construct scaffolds at room temperature, which results in the lowest thermal effect on printed products.

Moreover, surface roughness is one of the criteria in a 3D printing method or 3D printer evaluation [18, 20, 57, 58]. In addition, the surface roughness or surface topography is investigated as it has a significant effect on cell adhesion and proliferation in a positive way [61–63]. Patrício et al. found that PCL/PLA scaffolds fabricated by the SBD method had higher surface roughness and better cell adhesion than the m-FDM method for the same processing conditions and geometric evaluation [64]. They suggested that the main reason for this outcome was that the removal of the solvent in the post-processing caused the surface roughness in micro or submicron scales producing a positive effect on cell adhesion behavior. The surface topography is considered a subcriterion of the product quality criteria in this research work.

3.2 Usages

The usage and handling issues relating to the effective use of 3D printers include sterilization of printheads before and after printing, supplying material during printing, the requirement for post-processing, and toxicity for users or cells during fabrication [16]. From practical experience and experts' suggestions, sterilization much affects cell behavior. Therefore, all equipment that comes into direct contact with a printed sample should be disinfected before the printing process. This process is a crucial step that affects the purity of printed scaffolds. The same process is also applied after printing process is completed. Therefore, an SPM that can explicitly perform disinfection tasks has a higher priority. In addition, the ability to simply supply and replace materials during the printing process should be favorable for the 3D printers to fabricate the scaffold at actual size. Post-processing describes the process of the SPM required after printing, for example, the removal of solvents from the printed sample. Users and cells also need to be protected from harmful chemicals during the printing process. However, solvents such as chloroform or dichloromethane show a harmful effect on cells [65]. Thus, these solvents are required to be completely removed from the printed sample to avoid cytotoxicity. The post-processing might take several hours to remove the solvent in the scaffold before further treatment and testing [34, 55].

3.3 Productivity

Productivity is also important in all printing or machining processes. Productivity refers to process performance measurement such as production time, setup time, or large volume production capability [20, 66]. It is one of the major criteria

Table 2 The average printing accuracy and printing speed of different SPMs from the literature review

No	Printing method	Average printing ratio (δ_{PR})	Average printing precision (δ_{PE})	Average printing accuracy (δ_{PA})	Average printing speed (mm/s)
1	c-FDM	8.3%	8.7%	8.5%	24.3
2	s-FDM	9.4%	8.9%	9.1%	13.0
3	m-FDM	19.6%	11.6%	15.6%	4.0
4	SBD	21.8%	20.0%	20.9%	21.5

in practical applications for printing scaffolds at actual tissue size. Especially in bioprinting integration, reduction in printing time for hybrid construction is necessary to prevent cell damage because of living outside culture media. Table 2 also shows the average printing speed for different SPMs obtained from the literature review in Table 1. It can be seen that the c-FDM and SBD methods indicate the highest printing speeds compared with other methods. Besides printing time, the setup time, which includes the total time for heating and mixing materials or preparing the printhead, is also considered. Large size or high volume production is one of the evaluation criteria in conventional 3D printer selection [66, 67]. It is presented as the ability to continuously supply printing material to print large sizes or high volumes of tissues, hence, it is also an significant factor in practical tissue engineering applications.

3.4 Process economy

Process economy which is mentioned in most decision-making methods for 3D printing or machining process selection is the economic evaluation of printer and printing methods [20, 68]. The costs for materials, operations, and equipment should be all considered in this criterion. The material cost depends on the price of materials (commercial or customized material) used for each method. Table 3 shows the common PCL materials used for the SPMs in the literature review. PCL pellets are the most common type of material from commercial suppliers. PCL filament is not available from well-known manufacturers, including Sigma-Aldrich, Perstorp, and Polysciences. Pure or blended PCL filaments are customized material made by researchers at laboratories from commercial PCL powder or pellets [26, 39]. Thus, the c-FDM method with PCL filament as an input material type suffer a low priority in material compatibility.

Energy consumption costs (heat, compressed air, pump, etc.) or depreciation with different SPMs are also assessed as an operational investment. The FDM-based methods suffer energy losses due to printing with thermal energy while with compressed air methods, such as m-FDM or SBD, piping losses since using pneumatic operating equipment. In addition, the equipment investment refers to all equipment costs for the printhead only, not related to the printing table's drive mechanisms, is considered. The methods based on c-FDM and most of the s-FDM methods use stepper or servo motors for transferring material into the nozzle. Thus, the mechanism structures are simple and cost-effective. In contrast, the two other methods use compressed air to create pressure for material feeding. Therefore, additional equipment is required, such as a compressor, pressure regulator, a pipeline system, and specialized valves to stabilize the accuracy of closing and opening status of the material flow. Thus, the material feeding mechanism is more complex and expensive. However, the equipment costs for pneumatic systems can be shared with other pneumatic printheads to produce cost-reduction.

3.5 Flexibility

Flexibility is the ability to modify according to different situation, such as material combined with other materials or used in different forms [23]. Engineering tissues are made for different tissue types such as bone, cartilage, and skin. Thus, SPMs need to be compatible or rapidly convertible to use various materials. The variety and availability of raw materials for the SPMs are also an evaluated criterion. Only c-FDM has low material flexibility and few commercial material supply; the three other methods has various PCL-based material type choices. In addition, the ability of printhead in converting functions or combining with other printheads to expand the application scope of the method for bioprinting is also considered within the criterion of flexibility. Based on the literature review and practice, five evaluation criteria named product quality (PQ), usage issues (UI), productivity (PO), process economy (PE), and flexibility (FE) are proposed for SPM evaluation and selection, as shown in Table 4.

A group of experts from academia and hospital assessed the criteria and alternatives based on their experience and requirements. The respondents' identities are kept confidential upon request, and the survey results are used only to a limited extent in this study. A brief introduction and the requirements from the experts are described as follows:

User 1 — A specialist who works in a hospital's regenerative medicine center with many years of experience

Table 3 List of commercial PCL materials used in the literature review in Table 1

No	Name	Branch	Type	Code	Publication quantity
1	PCL-45,000	Sigma	Pellet	704105-500G	6
2	PCL-80,000	Sigma	Pellet	440744-500G	5
3	PCL-50,000	Polysciences	Pellet	26289–500	0
4	PCL-50,000	Polysciences	Powder	26090–500	2
5	PCL-80,000	Polysciences	Pellet	26290–500	1
6	PCL-50,000	Perstorp	Pellet	CAPA 6500	6
7	PCL-80,000	Perstorp	Pellet	CAPA 6800	2
8	PCL-80,000	Perstorp	Powder	CAPATM 6506	0
9	PCL 50,000	3D4Makers	Filament	FPCL1-0000–175-750-3D4M	2
10	PCL	None specific	Pellet	-	3
11	PCL	None specific	Filament	-	1

in research and work related to tissue engineering. PQ, UI, and PO are important criteria to accomplish this user's objectives.

User 2 — An academician working on different life science research fields, especially cell biology, molecular biology, and tissue engineering. The printing methods for this user require PQ, UI, and FE.

User 3 — An academician with much experience in using and constructing different 3D printers, scaffold fabrication, and tissue engineering research. The criteria most interesting to this user are PQ, UI, and PE.

Each user has different purposes for fabricating scaffold types and different requirements or criteria for 3D printing methods. Moreover, each scaffold type is compatible with several different SPMs due to the characteristics of each SPM. Thus, evaluating the priority of the SPMs for a specific scaffold type, including construction type or specific material type, is highly applicable. The evaluations are based on specific initial conditions to select the most suitable SPM for different applications using a multi-criteria assessment. It also makes sense to produce the commercial material in various types of 3D bio-printer construction for the tissue engineering field to achieve the multi-criteria purpose. An i-FAHP expert system integrating both selection criteria and evaluation criteria for selecting the most appropriate SPM is presented in this work. The system is designed with a user-friendly interface that allows users to utilize default assessment data collected from experts or to modify evaluation data to meet the specific requirements.

4 The i-FAHP approach for the multi-selection process

The i-FAHP method combines selection criteria and evaluation criteria in a unique model. There are different priorities of alternatives depending on the choice under the selection criteria while keeping the priorities unchanged in the evaluation criteria. This situation makes the i-FAHP model highly flexible and practical. It applies to complex problems with different initial conditions. The following sections describe the approach in more detail.

4.1 The i-FAHP structure construction

Figure 3 shows the hierarchical structure of the i-FAHP method. Based on a specific problem for evaluation, four main levels including goal, selection and evaluation criteria, sub-criteria, and alternatives are established. In the comparison to the conventional AHP model, the difference is the addition of selection criteria at the same level as evaluation criteria.

While the evaluation criteria for the alternatives are constant, the selection criteria change depending on the user's choices. The different combinations of sub-criteria under the selection criteria form the different conventional fuzzy-AHP models. Thus, the conventional fuzzy-AHP model turns into a specific case of the i-FAHP model.

4.2 The pair-wise comparison matrix generation

After constructing the hierarchical structure for the i-FAHP model, the pair-wise comparisons are established using linguistic terms, similar to the conventional fuzzy-AHP [69].

Table 5 shows the conversion of the linguistics scale to the reciprocal fuzzy scale using a triangular fuzzy number type. There are two kinds of pair-wise comparisons, criteria and alternative comparisons. While the criteria comparison evaluates the impact of each criterion compared to others in the pair-wise evaluation, the alternative comparison measures the impact of each alternative on others in the aspect of a specific criterion/sub-criterion.

The comparison matrix $\widetilde{A} = \left[\widetilde{a_{ij}}\right]$, where a fuzzy number is represented with three points as $\widetilde{a}_{ij}$, as presented in Eq. (2), in which $i, j = 1, 2, 3, \ldots, n$:

Table 4 Criteria and their descriptions

Main criterion	Sub-criterion	Descriptions
Product quality	Accuracy	The similarity between a final 3D printed model compared to the 3D designed model; the line width or pore size deviation
	Thermal effect	Long exposure to high temperature during the printing process leads to thermal degradation and thermal effects on material viscosity, flow rate and solidity time
	Surface topography	Surface nanoscale topography on the printed scaffold affects cell adhesion behavior
Usage issues	Sterilization	The equipment is easy to assemble and disassembly of parts for sterilization before and after the printing process
	Supply material	Ease of use in supplying or interchanging material
	Post-processing	Post-processing, such as solvent removal, required after the printing process
	Toxicity	Usage of harmful chemicals in the printing process
Productivity	Setup time	The process of preparing material for the printhead included mixing or heating materials
	Printing time	The time for printing a layer that is directly related to the printing speed
	Large volume	The ability to provide enough material over a long period for large product printing tasks
Process economy	Material waste	Dead or unused material after printing leads to material waste
	Material investment	The cost of material that depends on the popularity of the material form such as pellet, powder or filament PCL materials
	Operation investment	The cost related to the printing process operation, such as energy consumption and depreciation expenses
	Equipment investment	The cost associated with purchase or fabricating the 3D printer
Flexibility	Material flexibility	The wide range of different forms or combined with other materials
	Material availability	The ability to supply printing material from the commercial market
	Bioprinting integration	The ability to integrate with other bio-printheads or interchange with other material types for bioprinting

$$\widetilde{a_{ij}} = \begin{cases} \widetilde{f_{ii}} = (1,1,1) & if\ i = j \\ \widetilde{f_{ij}} = \left(a_{ij}, m_{ij}, b_{ij}\right) & if\ i \neq j \\ \widetilde{f_{ji}} = 1/\widetilde{f_{ij}} = \left(1/b_{ij}, 1/m_{ij}, 1/a_{ij}\right) & otherwise \end{cases} \quad (2)$$

The pair-wise comparison value for evaluation criteria depends on the experts' judgments. The pairwise comparison between the sub-selection criteria is determined according to which sub-selection criterion is selected. The fuzzy number $\widetilde{a_{ij}}$ between sub-selection criterion i and j is set to $\widetilde{9}$ if sub-selection criterion i is selected, and $\widetilde{1}$ for others, as shown in Eq. (3):

$$\widetilde{\mathrm{A}} = \begin{bmatrix} \widetilde{1} & \widetilde{9} & \widetilde{9} \\ 1/\widetilde{9} & \widetilde{1} & \widetilde{1} \\ 1/\widetilde{9} & \widetilde{1} & \widetilde{1} \end{bmatrix} = \begin{bmatrix} (1,1,1) & (8,9,9) & (8,9,9) \\ (1/9,1/9,1/8) & (1,1,1) & (1,1,1) \\ (1/9,1/9,1/8) & (1,1,1) & (1,1,1) \end{bmatrix} \quad (3)$$

Table 5 Linguistic scales and fuzzy-AHP membership functions

Fuzzy number ($\widetilde{f_{ij}}$)	Linguistic scales	Triangular fuzzy scale	Reciprocal fuzzy scale	Reciprocal fuzzy number ($1/\widetilde{f_{ij}}$)
$\widetilde{1}$	Equal	(1, 1, 1)	(1, 1, 1)	$1/\widetilde{1}$
$\widetilde{3}$	Moderate	(2, 3, 4)	(1/4, 1/3, 1/2)	$1/\widetilde{3}$
$\widetilde{5}$	Strong	(4, 5, 6)	(1/6, 1/5, 1/4)	$1/\widetilde{5}$
$\widetilde{7}$	Very strong	(6, 7, 8)	(1/8, 1/7, 1/6)	$1/\widetilde{7}$
$\widetilde{9}$	Extremely strong	(8, 9, 9)	(1/9, 1/9, 1/8)	$1/\widetilde{9}$
$\widetilde{2}$	The intermittent values between two adjacent scales	(1, 2, 3)	(1/3, 1/2, 1)	$1/\widetilde{2}$
$\widetilde{4}$		(3, 4, 5)	(1/5, 1/4, 1/3)	$1/\widetilde{4}$
$\widetilde{6}$		(5, 6, 7)	(1/7, 1/6, 1/5)	$1/\widetilde{6}$
$\widetilde{8}$		(7, 8, 9)	(1/9, 1/8, 1/7)	$1/\widetilde{8}$

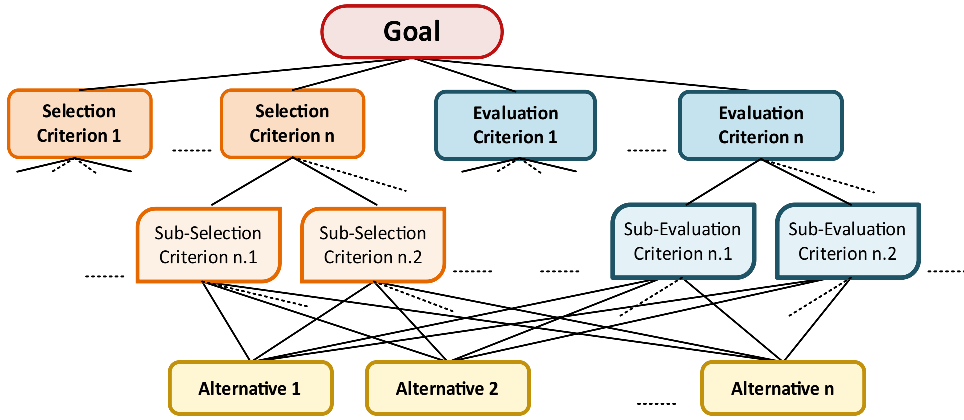

Fig. 3 The structure of the i-FAHP model

Thus, sub-selection criterion i is assigned the highest priority value among all sub-selection criteria. At the end of this stage, the consistency of each comparison matrix is checked using the consistency ratio ($\widetilde{CR}$). The consistency index ($\widetilde{CI}$) is calculated using the Eq. (4) to obtain the $\widetilde{CR}$ value using Eq. (5):

$$\widetilde{CI} = \frac{\widetilde{\lambda}_{max} - n}{n - 1} \quad (4)$$

$$\widetilde{CR} = \frac{\widetilde{CI}}{RI} \quad (5)$$

where $\widetilde{\lambda}_{max}$ is the fuzzy maximal eigenvalue of the average pair-wise comparison matrix; n is the size of the average pair-wise comparison matrix; RI is the random consistency index depending on the size of the comparison matrix [70]. If the $\widetilde{CR}$ is smaller than 0.1, the matrix is accepted regarding the consistency requirement. Otherwise, the pair-wise comparison values should be adjusted.

4.3 The final normalized weight determination

Since the consistency check is passed, the next step is to determine the geometric means $\widetilde{r}_i$ and fuzzy weights $\widetilde{fw}_i$ as given in Eqs. (6) and (7). The defuzzification of the fuzzy weights $\widetilde{M}_i$ is calculated by averaging the fuzzy weight $\widetilde{fw}_i$ for each criterion from Eq. (8). Finally, the normalized weight of each criterion $\widetilde{Nw}_i$ is also determined by normalizing values $\widetilde{M}_i$ as shown in Eq. (9)

$$\widetilde{r}_i = \left[\prod_{j=1}^{n} \widetilde{a}_{ij} \right]^{1/n} \quad (6)$$

$$\widetilde{fw}_i = \widetilde{r}_i \otimes \left[\sum_{j=1}^{n} \widetilde{r}_j \right]^{-1} = \left(aw_i, mw_i, bw_i \right) \quad (7)$$

$$\widetilde{M}_i = \frac{aw_i + mw_i + bw_i}{3} \quad (8)$$

$$\widetilde{Nw}_i = \frac{\widetilde{M}_i}{\sum_1^n \widetilde{M}_i} \quad (9)$$

5 Application of i-FAHP system for PCL-based SPM selection

The i-FAHP system for selecting the most potential PCL-based SPM is constructed and illustrated. Customized software helping decision-makers easily perform the pair-wise comparison, check the consistency of evaluation, produce multi-criteria evaluation results, and add and modify the criteria or alternatives for other specific applications is also introduced.

5.1 Development of i-FAHP structure

Based on the analysis from the literature review, practical experience of the research group and expert suggestions, the main criteria, sub-criteria, and alternatives are determined. The developed hierarchical structure of the SPM selection model is presented in Fig. 4. The decision hierarchy structure is composed of four levels. The top-level comprised the goal of selecting the most appropriate SPM method. The second level consisted of two selection criteria and five evaluation criteria. There are three sub-selection criteria under each selection criterion and three or four sub-evaluation criteria for each evaluation criterion. These sub-criteria are the third level of the hierarchy structure. The last level of the hierarchical structure includes four alternatives corresponding to four common SPM methods. Once the hierarchy is constructed, the pair-wise comparison matrix for each main criterion, sub-criterion is determined based on the integrated assessment of decision-makers, practical experience, and analysis from literature reviews. In the

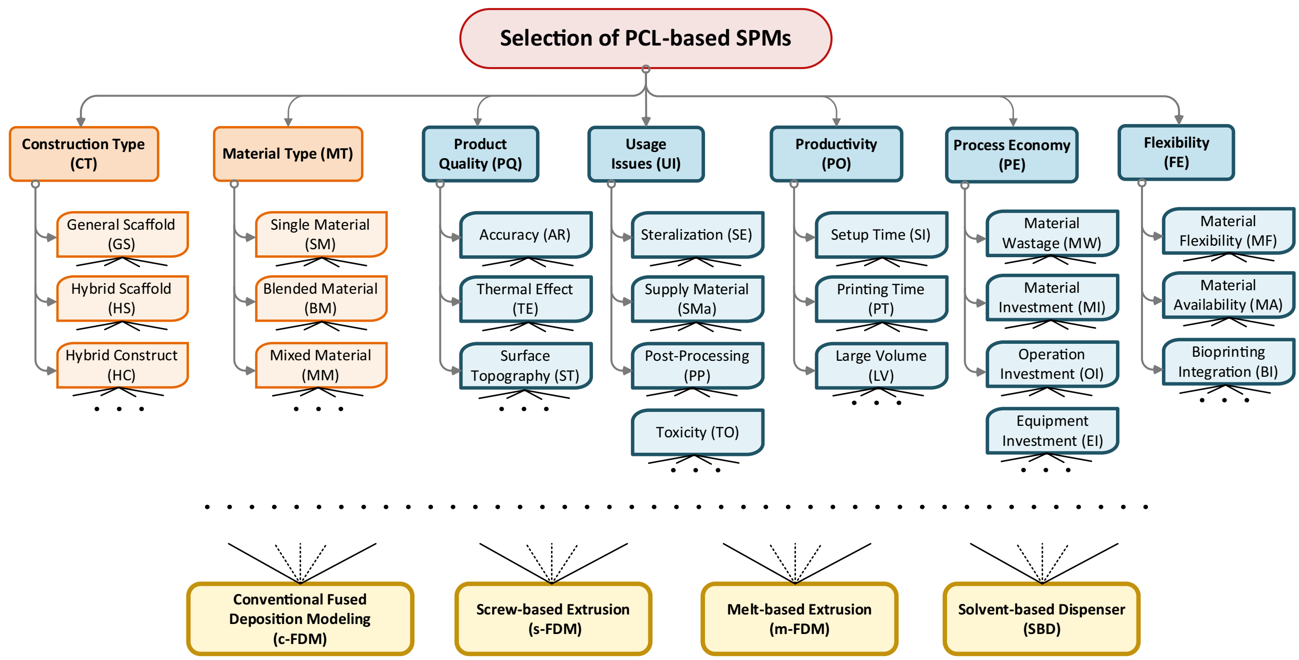

Fig. 4 The developed hierarchy structure for selecting the optimal PCL based-scaffold printing method

developed fuzzy-AHP model, the selection criteria normally have the highest impact compared to other evaluation criteria.

5.2 An illustrative example

As above mentioned, users are able to take advantage of the system to make their judgments on the criteria and sub-criteria priority for their usage. To illustrate the reliability and application of the i-FAHP system for selecting the optimal SPM, the assessment data of user 1 is introduced and analyzed. Table 6 represents the pair-wise comparison matrix of the main criteria for user 1. The user's main purpose is to effectively fabricate the HC type for tissue engineering applications. PQ, UI, and PO are the most important criteria among the five evaluation criteria to accomplish user 1's objectives. The consistency calculations in the comparison matrix are executed to ensure the acceptance of the judgments following Eqs. (4) and (5).

Based on the calculations in equations from Eqs. (6), (7), (8) and (9), the intermediate values and final normalized weight are shown in Table 7. In the conventional fuzzy-AHP method, the priority of alternatives is fixed because there is only specific case. In the i-FAHP for selecting the optimal SPMs, the alternatives' priority is different depending on the CT and MT selection. When one of CT or MT is selected, the comparison value between the selected CT or MT and other options is extremely strong compared to the others by setting 9 over the other types. Table 8 shows the pair-wise comparison of different selection sub-criteria in CT where the HC option is selected, the weight is set to $\widetilde{9}$ (8, 9, 9) to show the highest importance in comparison with other options which are set to $\widetilde{1}$ (1, 1, 1). As a result, the weight of HC is 0.812 which is much higher than other options with 0.094. In each sub-criterion, the pair-wise comparison matrix concerning the different alternatives is established based on analysis from the literature review and decision-makers. The pair-wise comparisons between SPMs that concern on the sub-criterion AR are determined in Table 9. The results of normalized weight calculation from Table 7

Table 6 Pair-wise comparison of the different main criteria

MC	CT	MT	PQ	UI	PO	PE	FE
CT	1, 1, 1	1, 1, 1	1, 2, 3	2, 3, 4	2, 3, 4	4, 5, 6	3, 4, 5
MT	1, 1, 1	1, 1, 1	1, 2, 3	2, 3, 4	2, 3, 4	4, 5, 6	3, 4, 5
PQ	1/3, 1/2, 1/1	1/3, 1/2, 1/1	1, 1, 1	1, 2, 3	1, 2, 3	3, 4, 5	2, 3, 4
UI	1/4, 1/3, 1/2	1/4, 1/3, 1/2	1/3, 1/2, 1/1	1, 1, 1	1, 2, 3	2, 3, 4	1, 2, 3
PO	1/4, 1/3, 1/2	1/4, 1/3, 1/2	1/3, 1/2, 1/1	1/3, 1/2, 1/1	1, 1, 1	1, 2, 3	1, 2, 3
PE	1/6, 1/5, 1/4	1/6, 1/5, 1/4	1/5, 1/4, 1/3	1/4, 1/3, 1/2	1/3, 1/2, 1/1	1, 1, 1	1/3, 1/2, 1/1
FE	1/5, 1/4, 1/3	1/5, 1/4, 1/3	1/4, 1/3, 1/2	1/3, 1/2, 1/1	1/3, 1/2, 1/1	1, 2, 3	1, 1, 1

Table 7 The geometric means, fuzzy weights, and normalized weights of the main criteria

MC	$\widetilde{r_i}$			$\widetilde{fw_i}$			$\widetilde{Nw_i}$
CT	1.739	2.318	2.826	0.151	0.269	0.455	0.258
MT	1.739	2.318	2.826	0.151	0.269	0.455	0.258
PQ	0.944	1.426	2.1	0.082	0.165	0.338	0.172
UI	0.635	0.944	1.369	0.055	0.109	0.22	0.113
PO	0.492	0.731	1.123	0.043	0.085	0.181	0.091
PE	0.285	0.363	0.521	0.025	0.042	0.084	0.044
FE	0.378	0.521	0.774	0.033	0.06	0.125	0.064

toTable 9 are aggregated into the corresponding rows MC, CT-HC, and AR in Table 10.

Similarity, the normalized weight of main criteria (MC), selection sub-criteria (SC-S), evaluation sub-criteria (SC-E), or alternatives (A) are summarized in Table 10. MC, SC-E, and A are fixed in the i-FAHP while SC-S including CT-x and MT-x is one of the three options respectively corresponding to each SC-S depending on the scaffold type selected at the early stage.

5.3 Results and discussion

The purpose of the i-FAHP method mainly focuses on to the determination of the most appropriate PCL-based SPM according to users' requirements for a specific application. Table 11 exhibits the results for evaluating the optimal SPM under different constrained CT and MT for user 1. The result shows that SBD is not recommended for printing scaffolds due to low scaffold accuracy and high material toxicity that can damage the cells compared with other methods. The m-FDM method is suggested for most scaffold types in HS and HC. However, it had lower priority in PQ and PO but higher priority in UI and FE. Under the GS selection criteria, where the weight of the SPM is the same (0.25 for each), the selection results are the most diverse.

Although possessing advantages in most aspects, the c-FDM method is only fitting for printhead that used pure PCL material due to the lack of variety and commercial supply of PCL based-material in filament form. The performance of a sensitivity analysis on the weights of the evaluation criteria is an important step to confirm the behavior of the i-FAHP method's validity problems. Since literature analysis and users' requirements all demonstrate PQ and UI as the most important evaluation criteria, therefore, these two criteria are grouped in analyzing sensitivity as a typical case. Eighty-one different calculations for this case in two types of sensitivity analysis are performed to compare the variations in the results. These calculations are conducted by changing the weight of each user's main criteria and among user-based requirements. For each user, the percentage in the change of selected criteria is determined. The amount of weight change is divided equally among the remaining criteria to ensure no difference in the total weight. The weight change for each criterion is normally from 15 to 30%. Figure 5 shows the sensitivity performance for user 1 in three cases: case 1 (no change all criteria weight); case 2 (decrease 20% for each PQ and UI, increase 28.6% for each PO, PE, and FE to keep constant total weight); case 3 (increase 20% for each PQ and UI, decrease 28.6% for each PO, PE, and FE).

Although, there is a slight change in the ranking of SPMs for ST3 and ST4 terms, no change in the highest priority in all cases could be observed. Figure 6 illustrates how the overall alternatives perform concerning three users' requirements. Three users have similar high priorities for PQ and UI but different priority for PO, FE, and PE. Thus, there are several variations in the weights among the main evaluation criteria and the sub-criteria according to their needs and usage requirements. The rankings of SPMs in the case from ST2 to ST4 and ST7 have a slight change for user 2 who needs higher flexibility than productivity and process economy for SPM; however, the highest priority SPM remains constant. The sensitivity analysis shows that the rank of the alternatives remains stable with criteria weight change for each user and all users. The result demonstrates that the priority established in the research work is reliable.

Table 8 The pair-wise comparison matrix of sub-criterion CT with HC selection

CT-HC	GS	HS	HC	Weight
GS	1, 1, 1	1, 1, 1	1/9, 1/9, 1/8	0.094
HS	1, 1, 1	1, 1, 1	1/9, 1/9, 1/8	0.094
HC	8, 9, 9	8, 9, 9	1, 1, 1	0.812

Table 9 The pair-wise comparison matrix of the different alternatives for sub-criterion AR

AR	c-FDM	s-FDM	m-FDM	SBD	Weight
c-FDM	1, 1, 1	1, 2, 3	3, 4, 5	6, 7, 8	0.488
s-FDM	1/3, 1/2, 1/1	1, 1, 1	2, 3, 4	5, 6, 7	0.326
m-FDM	1/5, 1/4, 1/3	1/4, 1/3, 1/2	1, 1, 1	2, 3, 4	0.131
SBD	1/8, 1/7, 1/6	1/7, 1/6, 1/5	1/4, 1/3, 1/2	1, 1, 1	0.055

Table 10 The priority values for all criteria, sub-criteria, and alternatives

Criterion	Symbol	C1	C2	C3	C4	C5	C6	C7	Type
MC	P0	0.258	0.258	0.172	0.113	0.091	0.044	0.064	MC
CT_GS	*P1_0*	*0.812*	*0.094*	*0.094*	-	-	-	-	*SC-S*
CT_HS	*P1_1*	*0.094*	*0.812*	*0.094*	-	-	-	-	*SC-S*
CT_HC	*P1_2*	*0.094*	*0.094*	*0.812*	-	-	-	-	*SC-S*
GS	P11	0.25	0.25	0.25	0.25	-	-	-	A
HS	P12	0.178	0.178	0.322	0.322	-	-	-	A
HC	P13	0.255	0.255	0.445	0.046	-	-	-	A
MT_SM	*P2_0*	*0.812*	*0.094*	*0.094*	-	-	-	-	*SC-S*
MT_BM	*P2_1*	*0.094*	*0.812*	*0.094*	-	-	-	-	*SC-S*
MT_MM	*P2_2*	*0.094*	*0.094*	*0.812*	-	-	-	-	*SC-S*
SM	P21	0.25	0.25	0.25	0.25	-	-	-	A
BM	P22	0.117	0.338	0.338	0.207	-	-	-	A
MM	P23	0.035	0.24	0.362	0.362	-	-	-	A
PQ	P3	0.665	0.167	0.167		-	-	-	SC-E
AR	P31	0.488	0.326	0.131	0.055	-	-	-	A
TE	P32	0.303	0.179	0.051	0.467	-	-	-	A
ST	P33	0.201	0.201	0.201	0.398	-	-	-	A
UI	P4	0.178	0.073	0.293	0.457	-	-	-	SC-E
SE	P41	0.294	0.083	0.162	0.46	-	-	-	A
SMa	P42	0.413	0.358	0.114	0.114	-	-	-	A
PP	P43	0.32	0.32	0.32	0.04	-	-	-	A
TO	P44	0.318	0.318	0.318	0.046	-	-	-	A
PO	P5	0.33	0.588	0.082	-	-	-	-	SC-E
SI	P51	0.45	0.335	0.077	0.138	-	-	-	A
PT	P52	0.47	0.175	0.068	0.288	-	-	-	A
LV	P53	0.466	0.347	0.074	0.113	-	-	-	A
PE	P6	0.38	0.38	0.148	0.093	-	-	-	SC-E
MW	P61	0.579	0.243	0.089	0.089	-	-	-	A
MI	P62	0.065	0.225	0.355	0.355	-	-	-	A
OI	P63	0.47	0.288	0.068	0.175	-	-	-	A
EI	P64	0.478	0.315	0.081	0.126	-	-	-	A
FE	P7	0.566	0.11	0.324	-	-	-	-	SC-E
MF	P71	0.083	0.219	0.349	0.349	-	-	-	A
MA	P72	0.054	0.229	0.359	0.359	-	-	-	A
BI	P73	0.091	0.091	0.534	0.284	-	-	-	A

MC main criterion, *SC-S* selection sub-criterion, *SC-E* evaluation sub-criterion, *A* alternative

5.4 Expert system for SPM method selection

The major purpose of expert system software is to provide a computer tool for decision-makers to quickly obtain a final result and flexibility. The expert system used in this research work is integrated with database management to well-build the hierarchy structure and apply this system to other similar problems. The software allows a user or decision-maker who is not an expert in theory calculation to easily and quickly obtain an evaluation result SPM method. The criteria and alternatives can be also added or removed from the user interface to quickly build and modify the hierarchy structure from decision-makers. The user selects a specific application in CT and MT in the initial step as shown in Fig. 7a. The alternatives are determined and modified depending on specific purpose, as appeared in Fig. 7b. Figure 8 presents a pair-wise comparison matrix interface for the main criteria. The decision-makers select each criterion or sub-criterion, pair-wise comparison matrix appears to assign judgments. The module requires that experts or users complete all pair-wise comparison matrices.

The consistency of the matrix is checked, and the priority is exhibited before moving to the next pair-wise comparison matrix. The pair-wise comparison matrix data for each user is saved with a data file in.xml format. After completing all comparison matrices, the

Table 11 The overall priority of different SPMs concerning the different scaffold type

Scaffold type	Selection criteria		Alternatives				First rank
	CT	MT	c-FDM	s-FDM	m-FDM	SBD	
ST1	GS	SM	0.289	0.254	0.235	0.223	c-FDM
ST2	GS	BM	0.264	0.27	0.251	0.215	s-FDM
ST3	GS	MM	0.249	0.252	0.255	0.244	m-FDM
ST4	HS	SM	0.275	0.24	0.248	0.236	c-FDM
ST5	HS	BM	0.251	0.257	0.264	0.228	m-FDM
ST6	HS	MM	0.236	0.238	0.269	0.257	m-FDM
ST7	HC	SM	0.29	0.254	0.271	0.185	c-FDM
ST8	HC	BM	0.265	0.271	0.287	0.177	m-FDM
ST9	HC	MM	0.25	0.253	0.292	0.206	m-FDM

priority for all criteria and the overall priorities for different SPMs are calculated. The final evaluation result is presented in Fig. 9 for the case of GS and BM. The sensitivity analysis is effortlessly performed by automatically collecting the results of the criterion weight change in the expert system. The developed expert system is a valuable tool for decision-makers to use or build their own i-FAHP model, check the consistency of their assessments, and effectively derive the final results. The developed software connected to the database with a friendly interface will help decision-makers conduct quickly, flexibly and accurately multi-criteria evaluations in SPM problems and similar multi-choice problems.

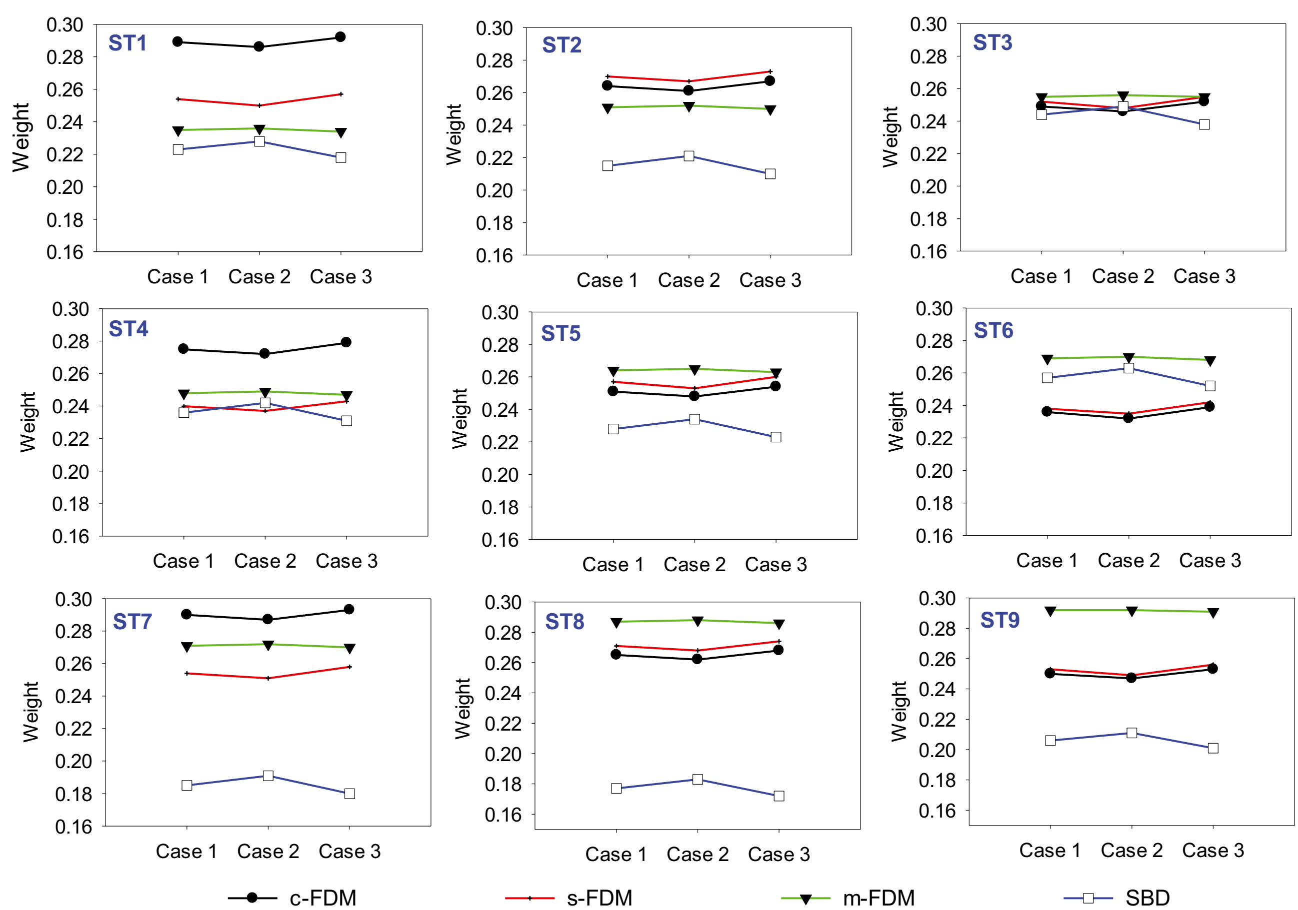

Fig. 5 Sensitivity analysis graph for user 1

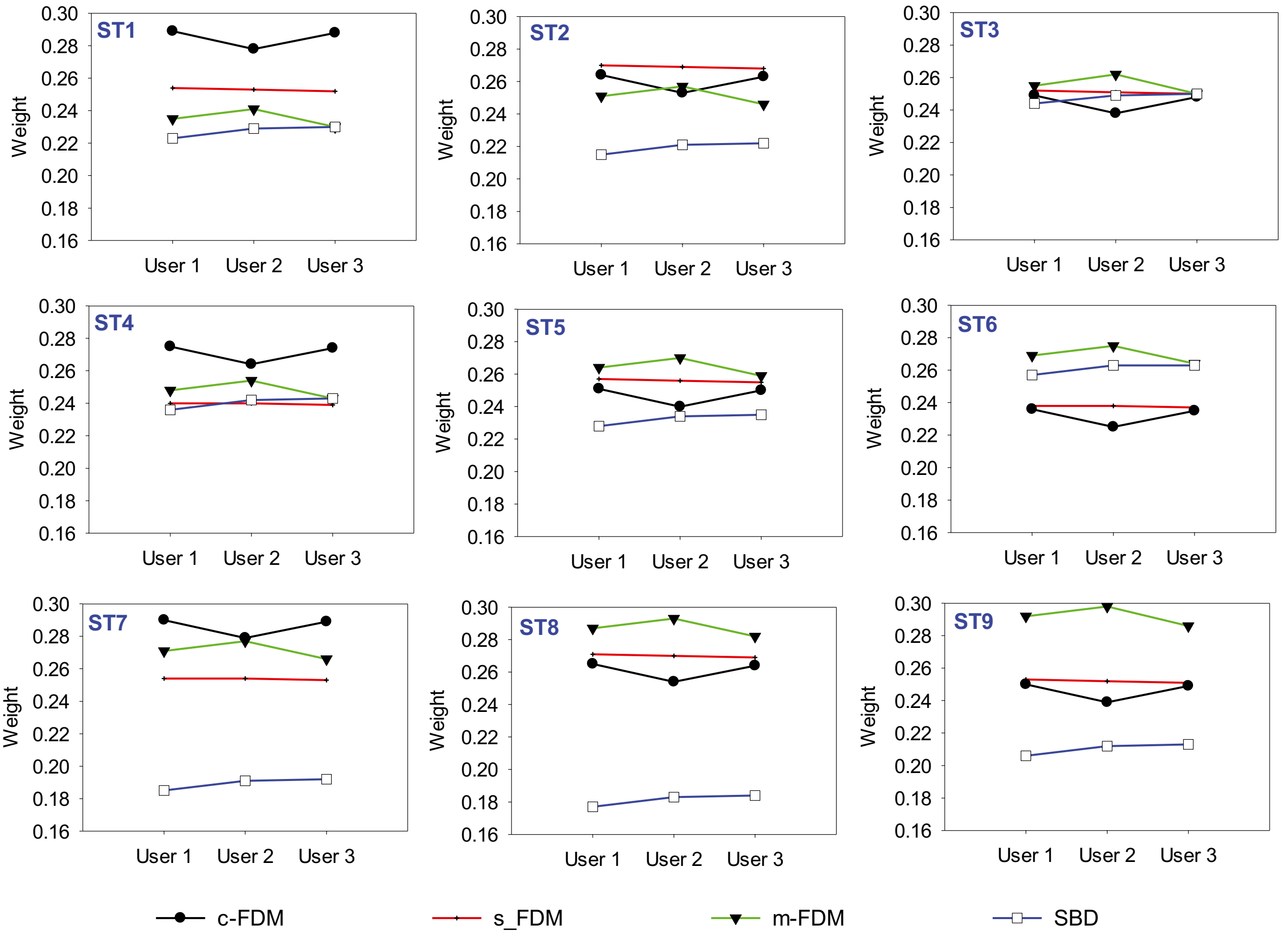

Fig. 6 Sensitivity analysis graph for different users

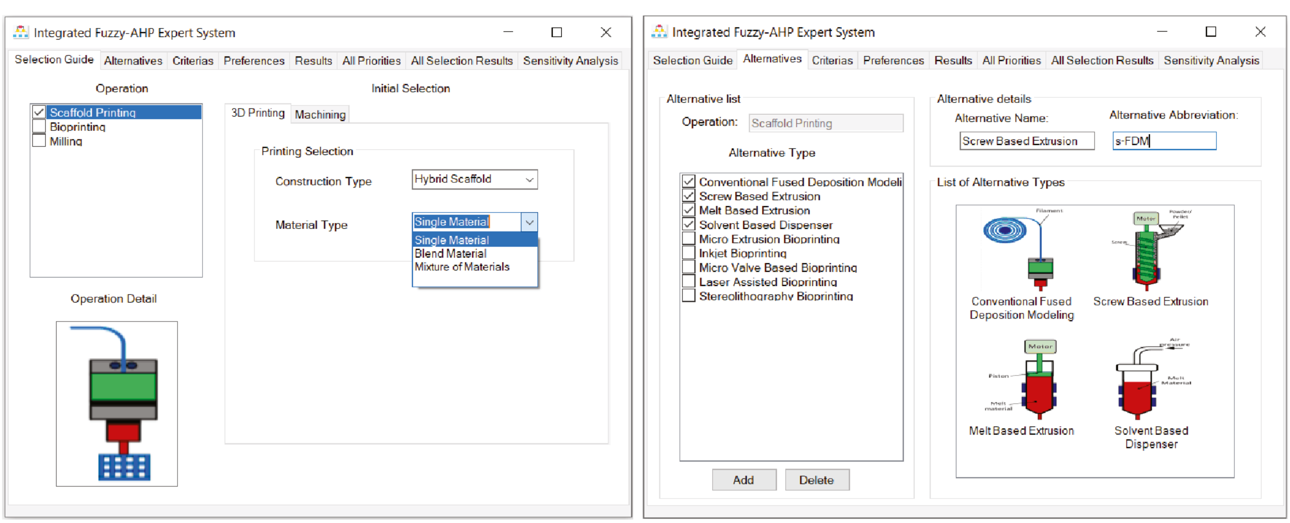

a) Initial scaffold type selection **b)** Alternative determination

Fig. 7 Input selection for fuzzy-AHP model. **a** Initial scaffold type selection. **b** Alternative determination

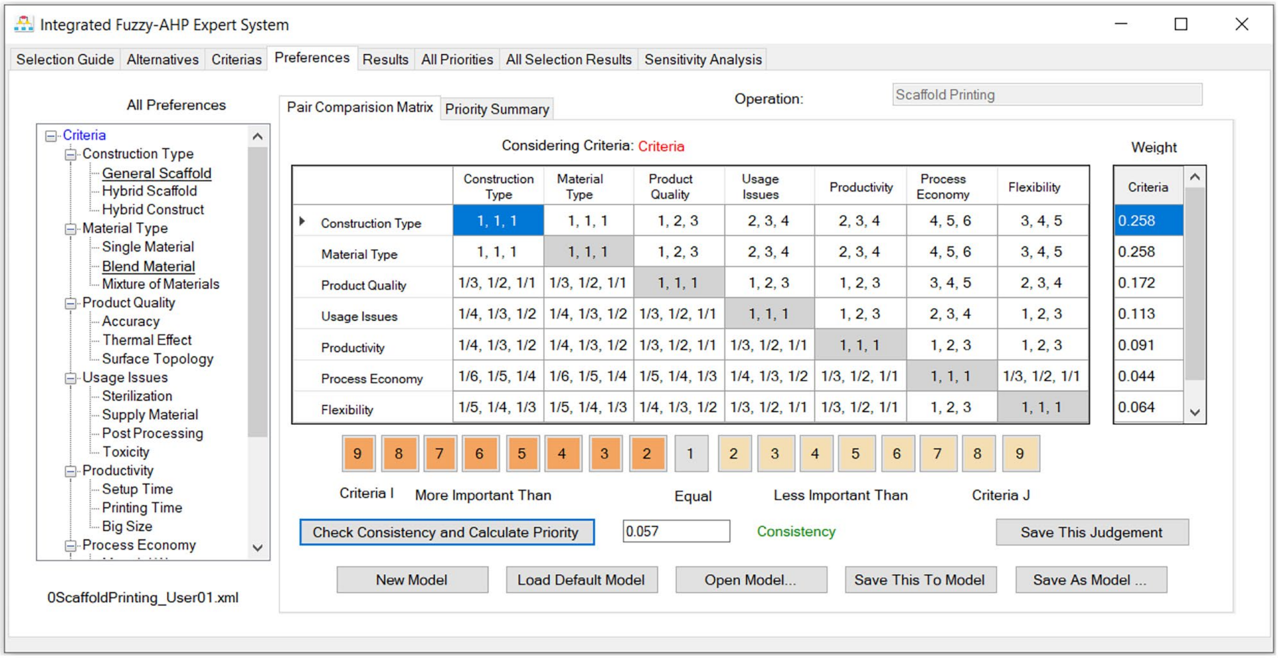

	Construction Type	Material Type	Product Quality	Usage Issues	Productivity	Process Economy	Flexibility	Criteria
Construction Type	1, 1, 1	1, 1, 1	1, 2, 3	2, 3, 4	2, 3, 4	4, 5, 6	3, 4, 5	0.258
Material Type	1, 1, 1	1, 1, 1	1, 2, 3	2, 3, 4	2, 3, 4	4, 5, 6	3, 4, 5	0.258
Product Quality	1/3, 1/2, 1/1	1/3, 1/2, 1/1	1, 1, 1	1, 2, 3	1, 2, 3	3, 4, 5	2, 3, 4	0.172
Usage Issues	1/4, 1/3, 1/2	1/4, 1/3, 1/2	1/3, 1/2, 1/1	1, 1, 1	1, 2, 3	2, 3, 4	1, 2, 3	0.113
Productivity	1/4, 1/3, 1/2	1/4, 1/3, 1/2	1/3, 1/2, 1/1	1/3, 1/2, 1/1	1, 1, 1	1, 2, 3	1, 2, 3	0.091
Process Economy	1/6, 1/5, 1/4	1/6, 1/5, 1/4	1/5, 1/4, 1/3	1/4, 1/3, 1/2	1/3, 1/2, 1/1	1, 1, 1	1/3, 1/2, 1/1	0.044
Flexibility	1/5, 1/4, 1/3	1/5, 1/4, 1/3	1/4, 1/3, 1/2	1/3, 1/2, 1/1	1/3, 1/2, 1/1	1, 2, 3	1, 1, 1	0.064

Fig. 8 The pair-wise comparison matrix for the main criteria

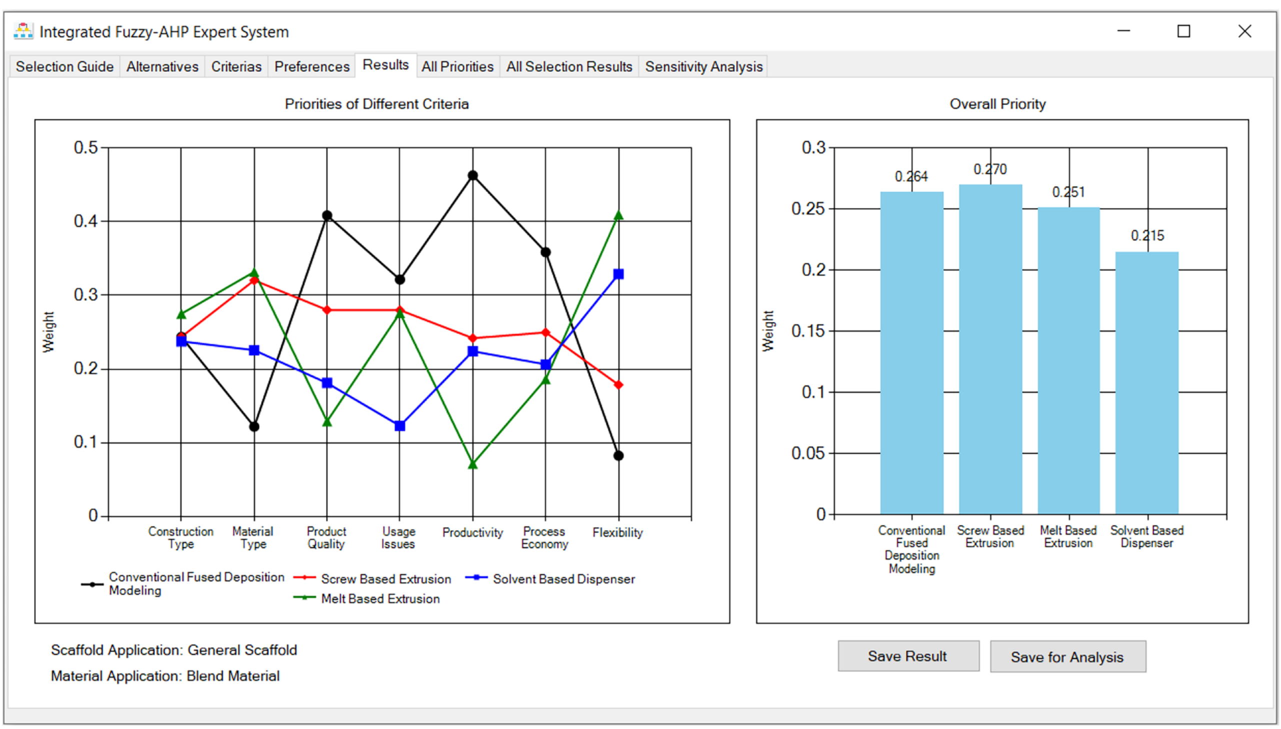

Fig. 9 The overall priority result for user 1 in the case of scaffold type ST2

6 Conclusions

The i-FAHP approach is proposed in this research work as the MCDM solution to evaluate PCL-based SPM. The selection and evaluation criteria are integrated into a single model and applied to build an expert system software tool to support decision-makers in choosing the most appropriate method for different initial selection of CT and MT. The assessments are constructed according to the judgments of experts, requirements of end-users, and the analysis from the literature review. A sensitivity analysis is carried out to evaluate the performance of the proposed model. The consistency test of comparison matrix and the sensitivity analysis ensured the reliability of the evaluation results. The following conclusions are drawn:

- The m-FDM method is the most appropriate for HS and HC for multi-materials while the c-FDM method is evaluated as the most desirable method for a SM in all CT.
- The expert system could help decision-makers to determine the highest priority of SPMs, to adjust the weight of specific criteria, and modify the hierarchy structure to modify the criteria for user purpose.
- These findings from this study will help construct the most appropriate bioprinter corresponding to specific tissue engineering application. The results also provide recommendations for supplying types of commercial PCL-based biomaterials in the market. The i-FAHP model could be considered with bioprinting method selection problem in future works.

Acknowledgements The authors gratefully acknowledge the efforts of experts and users for their assessments.

Author contribution All authors contributed to the study's conception and design. Lan Xuan Phung created the research direction, designed the methodology, reviewed the related works, and fabricated the expert system. Truong Do performed and collected the experts' judgments. Phuong Tran evaluated the methodology and system. Trung Kien Nguyen created the model's structure and made data analysis. All authors revised and approved the final manuscript.

Funding This research is funded by the Vingroup Innovation Foundation (VINIF) through project VINIF.2020.DA13.

Declarations

Competing interests The authors declare no competing interests.

References

1. Zhou X, Feng Y, Zhang J, Shi Y, Wang L (2020) Recent advances in additive manufacturing technology for bone tissue engineering scaffolds. Int J Adv Manuf Technol 108(11–12):3591–3606. https://doi.org/10.1007/s00170-020-05444-1
2. Bagde AD, Kuthe AM, Quazi S, Gupta V, Jaiswal S, Jyothilal S, Lande N, Nagdeve S (2019) State of the art technology for bone tissue engineering and drug delivery. Irbm 40(3):133–144. https://doi.org/10.1016/j.irbm.2019.03.001
3. Kang CW, Fang FZ (2018) State of the art of bioimplants manufacturing: part I. Adv Manuf 6(1):20–40. https://doi.org/10.1007/s40436-017-0207-4
4. Loh QL, Choong C (2013) Three-dimensional scaffolds for tissue engineering applications: role of porosity and pore size. Tissue Eng Part B Rev 19(6):485-. https://doi.org/10.1089/TEN.TEB.2012.0437
5. Borkar T, Goenka V, Jaiswal AK (2021) Application of poly-ε-caprolactone in extrusion-based bioprinting. Bioprinting. 21:e00111-e. https://doi.org/10.1016/J.BPRINT.2020.E00111
6. Kundu J, Shim J-H, Jang J, Kim S-W, Cho D-W (2015) An additive manufacturing-based PCL–alginate–chondrocyte bioprinted scaffold for cartilage tissue engineering. J Tissue Eng Regen Med 9(11):1286–1297. https://doi.org/10.1002/TERM.1682
7. Alagoz AS, Hasirci V (2019) 3D printing of polymeric tissue engineering scaffolds using open-source fused deposition modeling. Emergent Mater. https://doi.org/10.1007/s42247-019-00048-2
8. Cao T, Ho KH, Teoh SH (2003) Scaffold design and in vitro study of osteochondral coculture in a three-dimensional porous polycaprolactone scaffold fabricated by fused deposition modeling. Tissue Eng. 9(SUPPL. 1). https://doi.org/10.1089/10763270360697012
9. Shor L, Güçeri S, Wen X, Gandhi M, Sun W (2007) Fabrication of three-dimensional polycaprolactone/hydroxyapatite tissue scaffolds and osteoblast-scaffold interactions in vitro. Biomaterials 28(35):5291–5297. https://doi.org/10.1016/J.BIOMATERIALS.2007.08.018
10. Kim JY, Park EK, Kim S-Y, Shin J-W, Cho D-W (2008) Fabrication of a SFF-based three-dimensional scaffold using a precision deposition system in tissue engineering. J Micromech Microeng 18(5):055027-. https://doi.org/10.1088/0960-1317/18/5/055027
11. Gonçalves EM, Oliveira FJ, Silva RF, Neto MA, Fernandes MH, Amaral M, Vallet-Regí M, Vila M (2016) Three-dimensional printed PCL-hydroxyapatite scaffolds filled with CNTs for bone cell growth stimulation. J Biomed Mater Res B Appl Biomater 104(6):1210–1219. https://doi.org/10.1002/jbm.b.33432
12. Heo SJ, Kim SE, Wei J, Hyun YT, Yun HS, Kim DH, Shin JW, Shin JW (2009) Fabrication and characterization of novel nano- and micro-HA/PCL composite scaffolds using a modified rapid prototyping process. J Biomed Mater Res A 89(1):108–116. https://doi.org/10.1002/jbm.a.31726
13. Patrício T, Domingos M, Gloria A, D'Amora U, Coelho JF, Bártolo PJ (2014) Fabrication and characterisation of PCL and PCL/PLA scaffolds for tissue engineering. Rapid Prototyp J 20(2):145–156. https://doi.org/10.1108/RPJ-04-2012-0037
14. Kolan KCR, Li W, Semon JA, Day DE, Althage R, Leu M (2018) Solvent and melt based extrusion 3D printing of polycaprolactone bioactive glass composite for tissue engineering. Proceedings of the 3rd International Conference on Progress in Additive Manufacturing, Singapore 176–82. https://doi.org/10.25341/D4B018
15. Zimmerling A, Yazdanpanah Z, Cooper DML, Johnston JD, Chen X (2021) 3D printing PCL/nHA bone scaffolds: exploring the influence of material synthesis techniques. Biomater Res 25(1):1–12. https://doi.org/10.1186/S40824-021-00204-Y/TABLES/3
16. Andrea RC, Sinha R, Harings J, Bernaerts KV, Mota C, Moroni L (2021) Additive manufacturing using melt extruded thermoplastics for tissue engineering. Methods Mol Biol 2147:75–99. https://doi.org/10.1007/978-1-0716-0611-7_7
17. Marchewka J, Laska J (2020) Processing of poly-l-lactide and poly(l-lactide-co-trimethylene carbonate) blends by fused filament fabrication and fused granulate fabrication using RepRap 3D printer. Int J Adv Manuf Technol 106(11–12):4933–4944. https://doi.org/10.1007/s00170-020-04981-z

18. Moiduddin K, Mian SH, Alkhalefah H, Umer U (2019) Decision advisor based on uncertainty theories for the selection of rapid prototyping system. J Intell Fuzzy Syst 37(3):3897–3923. https://doi.org/10.3233/JIFS-190128
19. Yeh CC, Chen YF (2018) Critical success factors for adoption of 3D printing. Technol Forecast Soc Change 132(January):209–216. https://doi.org/10.1016/j.techfore.2018.02.003
20. Justino Netto JM, Ragoni IG, Frezzatto Santos LE, Silveira ZC (2019) Selecting low-cost 3D printers using the AHP method: a case study. SN Appl Sci 1(4). https://doi.org/10.1007/s42452-019-0352-4
21. Roy MK, Ray A, Pradhan BB (2014) Non-traditional machining process selection using integrated fuzzy AHP and QFD techniques: a customer perspective. Prod Manuf Res 2(1):530–549. https://doi.org/10.1080/21693277.2014.938276
22. Liu W, Zhu Z, Ye S (2020) A decision-making methodology integrated in product design for additive manufacturing process selection. Rapid Prototyp J 26(5):895–909. https://doi.org/10.1108/RPJ-06-2019-0174
23. Anand MB, Vinodh S (2016) Application of Fuzzy AHP – TOPSIS for ranking additive manufacturing process for microfabrication. Rapid Prototyp J 24(2):424–435. https://doi.org/10.1108/RPJ-10-2016-0160
24. Önüt S, Kara SS, Efendigil T (2008) A hybrid fuzzy MCDM approach to machine tool selection. J Intell Manuf 19(4):443–453. https://doi.org/10.1007/s10845-008-0095-3
25. Chen TCT, Lin YC (2021) Diverse three-dimensional printing capacity planning for manufacturers. Robot Comput Integr Manuf. 67(August). https://doi.org/10.1016/j.rcim.2020.102052
26. Izadifar Z, Chang T, Kulyk W, Chen X, Eames BF (2016) Analyzing biological performance of 3D-printed, cell-impregnated hybrid constructs for cartilage tissue engineering. Tissue Eng Part C Methods 22(3):173–188. https://doi.org/10.1089/ten.tec.2015.0307
27. Liu H, Ahlinder A, Yassin MA, Finne-Wistrand A, Gasser TC (2020) Computational and experimental characterization of 3D-printed PCL structures toward the design of soft biological tissue scaffolds. Mater Des 188:108488-. https://doi.org/10.1016/J.MATDES.2020.108488
28. Shim J-H, Kim JY, Park M, Park J, Cho D-W (2011) Development of a hybrid scaffold with synthetic biomaterials and hydrogel using solid freeform fabrication technology. Biofabrication 3(3):034102-. https://doi.org/10.1088/1758-5082/3/3/034102
29. Yu YZ, Zheng LL, Chen HP, Chen WH, Hu QX (2014) Fabrication of hierarchical polycaprolactone/gel scaffolds via combined 3D bioprinting and electrospinning for tissue engineering. Adv Manuf 2(3):231–238. https://doi.org/10.1007/s40436-014-0081-2
30. Ahn S, Kim Y, Lee H, Kim G (2012) A new hybrid scaffold constructed of solid freeform-fabricated PCL struts and collagen struts for bone tissue regeneration: fabrication, mechanical properties, and cellular activity. J Mater Chem 22(31). https://doi.org/10.1039/c2jm33310d
31. Kim G, Son J, Park S, Kim W (2008) Hybrid process for fabricating 3D hierarchical scaffolds combining rapid prototyping and electrospinning. Macromol Rapid Commun 29(19):1577–1581. https://doi.org/10.1002/marc.200800277
32. Kim JY, Lee TJ, Cho DW, Kim BS (2010) Solid free-form fabrication-based PCL/HA scaffolds fabricated with a multi-head deposition system for bone tissue engineering. J Biomater Sci Polym Ed 21(6–7):951–962. https://doi.org/10.1163/156856209X458380
33. Schipani R, Nolan DR, Lally C, Kelly DJ (2020) Integrating finite element modelling and 3D printing to engineer biomimetic polymeric scaffolds for tissue engineering. Connect Tissue Res 61(2):174–189. https://doi.org/10.1080/03008207.2019.1656720
34. Choi JW, Lee K, Koh YH, Kim HE (2020) Novel poly(ε-caprolactone) scaffolds comprised of tailored core/shell-structured filaments using 3D plotting technique. Mater Lett 269:127659-. https://doi.org/10.1016/J.MATLET.2020.127659
35. Beatrice CAG, Shimomura KMB, Backes EH, Harb SV, Costa LC, Passador FR, Pessan LA (2021) Engineering printable composites of poly (ε-polycaprolactone) / β-tricalcium phosphate for biomedical applications. Polym Compos 42(3):1198–1213. https://doi.org/10.1002/pc.25893
36. Dávila JL, Freitas MS, Inforçatti Neto P, Silveira ZC, Silva JVL, D'Ávila MA (2016) Fabrication of PCL/β-TCP scaffolds by 3D mini-screw extrusion printing. J Appl Polym Sci 133(15):1–9. https://doi.org/10.1002/app.43031
37. Aydogdu MO, Mutlu B, Kurt M, Inan AT, Kuruca SE, Erdemir G, Sahin YM, Ekren N, Oktar FN (2019) Gunduz O (2019) Developments of 3D polycaprolactone/beta-tricalcium phosphate/collagen scaffolds for hard tissue engineering. J Aust Ceram Soc 55(3):849–855. https://doi.org/10.1007/S41779-018-00299-Y
38. Albrecht LD, Sawyer SW, Soman P (2016) Developing 3D scaffolds in the field of tissue engineering to treat complex bone defects. 3D Print Addit Manuf 3(2):106–112. https://doi.org/10.1089/3DP.2016.0006
39. Hutmacher DW, Schantz T, Zein I, Ng KW, Teoh SH, Tan KC (2001) Mechanical properties and cell cultural response of polycaprolactone scaffolds designed and fabricated via fused deposition modeling. J Biomed Mater Res 55(2):203–216. https://doi.org/10.1002/1097-4636(200105)55:2%3c203::AID-JBM1007%3e3.0.CO;2-7
40. Liu F, Vyas C, Poologasundarampillai G, Pape I, Hinduja S, Mirihanage W, Bartolo PJ (2018) Process-driven microstructure control in melt-extrusion-based 3D printing for tailorable mechanical properties in a polycaprolactone filament. Macromol Mater Eng 303(8):1800173-. https://doi.org/10.1002/MAME.201800173
41. Justino Netto JM, Idogava HT, Frezzatto Santos LE, Silveira Z, d C, Romio P, Alves J L, (2021) Screw-assisted 3D printing with granulated materials: a systematic review. Int J Adv Manuf Technol 115(9–10):2711–2727. https://doi.org/10.1007/s00170-021-07365-z
42. Jo S, Kang SM, Park SA, Kim WD, Kwak J, Lee H (2013) Enhanced adhesion of preosteoblasts inside 3D PCL scaffolds by polydopamine coating and mineralization. Macromol Biosci 13(10):1389–1395. https://doi.org/10.1002/MABI.201300203
43. Declercq HA, Desmet T, Dubruel P, Cornelissen MJ (2014) The role of scaffold architecture and composition on the bone formation by adipose-derived stem cells. Tissue Eng Part A 20(1–2):434–444. https://doi.org/10.1089/ten.tea.2013.0179
44. Yong LC, Malek NFA, Yong ENS, Yap WH, Nobuyuki M, Yoshitaka N (2019) Fabrication of hydroxyapatite blended cyclic type polylactic acid and poly (ε-caprolactone) tissue engineering scaffold. Int J Appl Ceram Technol 16(2):455–461. https://doi.org/10.1111/IJAC.13115
45. Kim JY, Jin G-Z, Park IS, Kim J-N, Chun SY, Park EK, Kim S-Y, Yoo J, Kim S-H, Rhie J-W, Cho D-W (2010) Evaluation of solid free-form fabrication-based scaffolds seeded with osteoblasts and human umbilical vein endothelial cells for use in vivo osteogenesis. Tissue Eng Part A 16(7):2229–2236. https://doi.org/10.1089/TEN.TEA.2009.0644
46. Murphy C, Kolan K, Li W, Semon J, Day D, Leu M (2017) 3D bioprinting of stem cells and polymer/bioactive glass composite scaffolds for bone tissue engineering. Int J Bioprint 3(1):53–63. https://doi.org/10.18063/IJB.2017.01.005
47. Siddiqui N, Asawa S, Birru B, Baadhe R (2018) Rao S (2018) PCL-based composite scaffold matrices for tissue engineering applications. Mol Biotechnol 60(7):506–532. https://doi.org/10.1007/S12033-018-0084-5
48. Cubo-Mateo N, Rodríguez-Lorenzo LM (2020) Design of thermoplastic 3D-printed scaffolds for bone tissue engineering: influence of parameters of "Hidden" importance in the physical properties of scaffolds. Polymers (Basel) 12(7):1546

49. Luo W, Zhang S, Lan Y, Huang C, Wang C, Lai X, Chen H, Ao N (2018) 3D printed porous polycaprolactone/oyster shell powder (PCL/OSP) scaffolds for bone tissue engineering. Mater Res Express 5(4):045403. https://doi.org/10.1088/2053-1591/AAB916
50. Hou Y, Wang W, Bártolo P (2020) Novel poly(ε-caprolactone)/graphene scaffolds for bone cancer treatment and bone regeneration. 3D Print Addit Manuf 7(5):222–229. https://doi.org/10.1089/3DP.2020.0051
51. Huang B, Vyas C, Roberts I, Poutrel QA, Chiang WH, Blaker JJ, Huang Z, Bártolo P (2019) Fabrication and characterisation of 3D printed MWCNT composite porous scaffolds for bone regeneration. Mater Sci Eng C 98:266–278. https://doi.org/10.1016/j.msec.2018.12.100
52. Jiang CP, Huang JR, Hsieh MF (2011) Fabrication of synthesized PCL-PEG-PCL tissue engineering scaffolds using an air pressure-aided deposition system. Rapid Prototyp J 17(4):288–297. https://doi.org/10.1108/13552541111138414
53. Buyuksungur S, Hasirci V, Hasirci N (2021) 3D printed hybrid bone constructs of PCL and dental pulp stem cells loaded GelMA. J Biomed Mater Res A 109(12):2425–2437. https://doi.org/10.1002/jbm.a.37235
54. Kim YB, Lee H, Yang GH, Choi CH, Lee D, Hwang H, Jung WK, Yoon H, Kim GH (2016) Mechanically reinforced cell-laden scaffolds formed using alginate-based bioink printed onto the surface of a PCL/alginate mesh structure for regeneration of hard tissue. J Colloid Interface Sci 461:359–368. https://doi.org/10.1016/j.jcis.2015.09.044
55. Li Y, Yu Z, Ai F, Wu C, Zhou K, Cao C, Li W (2021) Characterization and evaluation of polycaprolactone/hydroxyapatite composite scaffolds with extra surface morphology by cryogenic printing for bone tissue engineering. Mater Des 205:109712. https://doi.org/10.1016/j.matdes.2021.109712
56. Kolan KCR, Semon JA, Bromet B, Day D, Leu MC (2019) Bioprinting with human stem cell-laden alginate-gelatin bioink and bioactive glass for tissue engineering. Int J Bioprint 5(2.2 Special Issue):3–15. https://doi.org/10.18063/ijb.v5i2.2.204
57. Peko I, BajiĆ D, VeŽA I (2015) Selection of additive manufacturing process using the AHP method. International conference: mechanical technologies and structural materials (2018):119–129. https://doi.org/10.13140/RG.2.1.2713.2246
58. Wang Y, Zhong RY, Xu X (2018) A decision support system for additive manufacturing process selection using a hybrid multiple criteria decision-making method. Rapid Prototyp J 24(9):1544–1553. https://doi.org/10.1108/RPJ-01-2018-0002
59. Chen TCT, Lin YC (2020) A FAHP-FTOPSIS approach for bioprinter selection. Health Technol (Berl) 10(6):1455–1467. https://doi.org/10.1007/s12553-020-00469-8
60. Mohamed OA, Masood SH, Bhowmik JL (2015) Optimization of fused deposition modeling process parameters: a review of current research and future prospects. Adv Manuf 3(1):42–53. https://doi.org/10.1007/s40436-014-0097-7
61. Cai S, Wu C, Yang W, Liang W, Yu H, Liu L (2020) Recent advance in surface modification for regulating cell adhesion and behaviors. Nanotechnol Rev 9(1):971–989. https://doi.org/10.1515/ntrev-2020-0076
62. Anselme K, Ploux L, Ponche A (2010) Cell/material interfaces: Influence of surface chemistry and surface topography on cell adhesion. J Adhes Sci Technol 24(5):831–852. https://doi.org/10.1163/016942409X12598231568186
63. Zhou J, Zhang X, Sun J, Dang Z, Li J, Li X, Chen T (2018) The effects of surface topography of nanostructure arrays on cell adhesion. Phys Chem Chem Phys 20(35):22946–22951. https://doi.org/10.1039/C8CP03538E
64. Patrício T, Domingos M, Gloria A, Bártolo P (2013) Characterisation of PCL and PCL/PLA scaffolds for tissue engineering. Procedia CIRP 5:110–114. https://doi.org/10.1016/j.procir.2013.01.022
65. Vogt L, Rivera LR, Liverani L, Piegat A, El Fray M, Boccaccini AR (2019) Poly(epsilon-caprolactone)/poly(glycerol sebacate) electrospun scaffolds for cardiac tissue engineering using benign solvents. Mater Sci Eng C Mater Biol Appl 103:109712. https://doi.org/10.1016/j.msec.2019.04.091
66. Çentinkaya C, Kabak M, Özceylan E (2017) 3D printer selection by using fuzzy analytic hierarchy process and PROMETHEE. Bilişim Teknolojileri Dergisi 371–380. https://doi.org/10.17671/gazibtd.347610
67. Prabhu SR, Ilangkumaran M (2019) Selection of 3D printer based on FAHP integrated with GRA-TOPSIS. Int J Mater Prod Technol 58(2–3):155–177. https://doi.org/10.1504/IJMPT.2019.097667
68. Kadkhoda-Ahmadi S, Hassan A, Asadollahi-Yazdi E (2019) Process and resource selection methodology in design for additive manufacturing. Int J Adv Manuf Technol 104(5–8):2013–2029. https://doi.org/10.1007/s00170-019-03991-w
69. Chang TH, Wang TC (2009) Using the fuzzy multi-criteria decision making approach for measuring the possibility of successful knowledge management. Inf Sci 179(4):355–370. https://doi.org/10.1016/j.ins.2008.10.012
70. Saaty RW (1987) The analytic hierarchy process-what it is and how it is used. Math Model 9(3–5):161–176. https://doi.org/10.1016/0270-0255(87)90473-8

Publisher's Note Springer Nature remains neutral with regard to jurisdictional claims in published maps and institutional affiliations.